DMD Fast Forward. Published on June 4, 2024 as DOI: 10.1124/dmd.124.001688
This article has not been copyedited and formatted. The final version may differ from this version.

Mass balance, metabolic pathways, absolute bioavailability, and pharmacokinetics of giredestrant in healthy subjects

Smita Kshirsagar, Ya-Chi Chen, Jiajie Yu, Mary R. Gates, Sonoko Kawakatsu, S Cyrus Khojasteh, Shuguang Ma,† Luna Musib,† Vikram Malhi, Uyi Osaghae, Jing Wang, Sungjoon Cho, Yang (Thomas) Tang, Donglu Zhang, Weiping Zhao, Tom De Bruyn†

Clinical Pharmacology, Genentech, Inc., South San Francisco, California (S.K., Y.C.C., J.Y., S.Ka., L.M., V.M.)

Drug Metabolism and Pharmacokinetics, Genentech, Inc., South San Francisco, California (S.C.K., S.M., J.W., S.C., Y.T., D.Z., W.Z., T.DB.)

Early Clinical Development, Oncology, Genentech, Inc., South San Francisco, California (M.R.G.)

Safety Science, Genentech, Inc., South San Francisco, California (U.O.)

†At the time the study was conducted.

DMD Fast Forward. Published on June 4, 2024 as DOI: 10.1124/dmd.124.001688
This article has not been copyedited and formatted. The final version may differ from this version.

Running Title: Absorption, Metabolism and Excretion of Giredestrant

Corresponding author: Tom De Bruyn, PhD, Department of Drug Metabolism and Pharmacokinetics, Genentech Inc., 1 DNA Way, South San Francisco, CA 94080, USA. Email: tomdebruyn788@gmail.com, Telephone number: +1 4155309457

Additional Co-corresponding author: Weiping Zhao, Department of Drug Metabolism and Pharmacokinetics, Genentech Inc., 1 DNA Way, South San Francisco, CA 94080, USA. Email: zhaow33@gene.com

Number of text pages: 47

Number of Tables: 4

Number of Figures: 6

Number of References: 16

Number of words in Abstract: 246

Number of words in Introduction: 485

Number of words in Discussion: 1299

List of nonstandard abbreviations:

1-aminobenzotriazole (ABT), absolute bioavailability (aBA), absorption, distribution, metabolism, and excretion (ADME), adverse events (AEs), AEs of special interest (AESIs), Amount excreted (Ae), below the limit of quantitation (BLQ), confidence interval (CI), electrospray ionization (ESI), enterohepatic recirculation (EHR), equivalents (eq), ER positive (ER+), estrogen receptor 1 (*ESR1)*, estrogen receptor

DMD Fast Forward. Published on June 4, 2024 as DOI: 10.1124/dmd.124.001688
This article has not been copyedited and formatted. The final version may differ from this version.

alpha (Erα), estrogen receptors (ER), Fraction excreted (Fe), Fraction escaping gut metabolism (Fg), Fraction escaping hepatic metabolism (Fh), fraction absorbed in human (Fa), fraction metabolized (Fm), geometric mean ratio (GMR), Good Clinical Practice (GCP), high-performance liquid chromatography (HPLC), intestinal re-absorption (IR), International Council for Harmonisation (ICH), liquid chromatography (LC), liquid scintillation counting (LSC), lower limit of quantification (LLOQ), median time to maximum concentration (T_{max}), millisievert (mSv), Multiple Reaction Monitoring (MRM), once daily (QD), pharmacokinetic (PK), serious AEs (SAEs), tandem mass spectrometry (MS/MS), total radioactivity (TR), women of non-childbearing potential (WNCBP)

DMD Fast Forward. Published on June 4, 2024 as DOI: 10.1124/dmd.124.001688
This article has not been copyedited and formatted. The final version may differ from this version.

Abstract

Giredestrant is a potent and selective small molecule estrogen receptor degrader. The objectives of this study were to assess the absolute bioavailability (aBA) of giredestrant and to determine the mass balance, routes of elimination and metabolite profile of [^{14}C]giredestrant. In Part 1 (mass balance), a single 30.8 mg oral dose of [^{14}C]giredestrant (105 µCi) was administered to women of non-childbearing potential (WNCBP, n = 6). The mean recovery of total radioactivity (TR) in excreta was 77.0%, with 68.0% of the dose excreted in feces and 9.04% excreted in urine over a 42-day sample collection period. The majority of the circulating radioactivity (56.8%) in plasma was associated with giredestrant. Giredestrant was extensively metabolized with giredestrant representing only 20.0% and 1.90% of the dose in feces and urine, respectively. All metabolites in feces resulted from oxidative metabolism and represented 44.7% of the dose. In Part 2 (absolute bioavailability, aBA), WNCBP (n = 10) received an oral (30 mg capsule) or intravenous (30 mg solution) dose of giredestrant. The aBA of giredestrant after oral administration was 58.7%. Following the intravenous dose, giredestrant had a plasma clearance and volume of distribution of 5.31 L/h and 266 L, respectively. In summary, giredestrant was well tolerated, rapidly absorbed, and showed moderate oral bioavailability with low recovery of the dose as parent drug in excreta. Oxidative metabolism followed by excretion in feces was identified as the major route of elimination of giredestrant.

DMD Fast Forward. Published on June 4, 2024 as DOI: 10.1124/dmd.124.001688
This article has not been copyedited and formatted. The final version may differ from this version.

Significance statement:

This study provides definitive insight into the absorption, distribution, metabolism, and excretion of giredestrant in humans. The results show that giredestrant exhibits low clearance, high volume of distribution, and moderate oral bioavailability in humans. In addition, the data show that oxidative metabolism followed by excretion in feces is the primary elimination route of giredestrant in humans. These results will be used to further inform the clinical development of giredestrant.

Clinical trial registration (ClinicalTrials.gov): NCT04680273

DMD Fast Forward. Published on June 4, 2024 as DOI: 10.1124/dmd.124.001688
This article has not been copyedited and formatted. The final version may differ from this version.

Introduction

Breast cancer is the most commonly diagnosed cancer in women, with an estimated global incidence of over 2 million new cases and 0.6 million deaths reported in 2020 (Sung et al., 2021). Approximately 80% of all breast cancers express estrogen receptors (ER) and the vast majority of these cancers are dependent on the ER for tumor growth and progression. Modulation of estrogen activity and/or synthesis is the mainstay of therapeutic approaches in women with ER positive (ER+) breast cancer. However, despite the effectiveness of available endocrine therapies such as ER antagonists (e.g., tamoxifen), aromatase inhibitors (e.g., anastrozole, letrozole, and exemestane), and full ER antagonists/degraders (e.g., fulvestrant), many patients ultimately relapse or develop resistance to these agents and therefore require further treatment for optimal disease control. Mutations in the estrogen receptor 1 (*ESR1)* gene that encodes estrogen receptor alpha (ERα) appear to be a major mechanism of acquired resistance to aromatase inhibitors and are associated with poorer outcomes (Schiavon et al., 2015; Chandarlapaty et al., 2016; Fribbens et al., 2016).

Giredestrant is a potent, orally bioavailable, small molecule therapeutic agent that is being developed for the treatment of patients with ER+ breast cancer. Giredestrant antagonizes the effects of estrogen via competitive binding to the ligand-binding domain of both wild-type and mutant ER with nanomolar biochemical potency. In addition, giredestrant reduces levels of ERα protein through proteasome-mediated degradation. Degradation of the ER is hypothesized to enable full suppression of ER signaling, which is not achieved by first generation ER therapeutics such as tamoxifen, which display partial agonism (Guan et al., 2019). Giredestrant is currently being evaluated in multiple

DMD Fast Forward. Published on June 4, 2024 as DOI: 10.1124/dmd.124.001688
This article has not been copyedited and formatted. The final version may differ from this version.

Phase 2 and Phase 3 clinical trials for both early and advanced stage breast cancer and has demonstrated encouraging clinical activity in patients with hormone receptor-positive advanced or metastatic breast cancer, independent of *ESR1* mutations (Jhaveri et al., 2021; Jhaveri et al., 2023).

The single and multiple-dose pharmacokinetics of giredestrant following oral administration in patients with ER+, human epidermal growth factor receptor 2 (HER2)-negative, locally advanced/metastatic breast cancer have been evaluated previously (Study NCT03332797; Malhi et al., 2023). Following single-dose oral administration, giredestrant was rapidly absorbed with a median time to maximum concentration (T_{max}) of 1.75 to 3.13 hours and exhibited dose-proportional increase in exposure at doses ranging from 10 mg to 250 mg. At the clinical dose of 30 mg, the mean plasma half-life was 43.0 hours, supporting once-daily dosing.

The objectives of the current study were to determine the mass balance and routes of elimination of giredestrant and characterize the metabolites of giredestrant in human plasma, urine, and feces following a single dose of [^{14}C]giredestrant. In addition, the study aimed to characterize the pharmacokinetics and absolute bioavailability of giredestrant following oral and intravenous (IV) administration. Overall, this study provides quantitative and mechanistic information on the absorption, distribution, metabolism, and excretion (ADME) of giredestrant in humans.

DMD Fast Forward. Published on June 4, 2024 as DOI: 10.1124/dmd.124.001688
This article has not been copyedited and formatted. The final version may differ from this version.

Materials and Methods

Study design:

This clinical trial was an open-label, two-part study in healthy female subjects of non-childbearing potential (WNCBP) and conducted at a single center in the UK (Quotient Sciences, Nottingham, UK). This study was conducted in full conformance with the International Council for Harmonisation of Technical Requirements for Pharmaceuticals for Human Use (ICH), E6 Guideline for Good Clinical Practice (GCP), the principles of the Declaration of Helsinki, and applicable laws and regulations of the country in which the research was conducted (i.e., the U.K.). The study complied with the requirements of the ICH E2A guidelines (Clinical Safety Data Management: Definitions and Standards for Expedited Reporting) and the E.U. Clinical Trial Directive 2001/20/EC and applicable local, regional, and national laws. The study protocol, and its amendments, and the informed consent forms were submitted for review and approval by the Health and Social Care Research Ethics Committee A (Lisburn, UK).

The evaluation of giredestrant TR concentrations was performed at Pharmaron UK Ltd. (Northamptonshire, UK), plasma concentrations of giredestrant were evaluated by Covance Laboratories Inc. (Madison, WI, USA), and the metabolite profiling and identification analyses were performed at Genentech Inc. (South San Francisco, CA, USA).

Part 1 of the study was an open-label, single-treatment mass balance study. The subjects were admitted to the clinic the afternoon before the first day of drug

DMD Fast Forward. Published on June 4, 2024 as DOI: 10.1124/dmd.124.001688
This article has not been copyedited and formatted. The final version may differ from this version.

administration. On Day 1 of the study, participants were dosed with a single oral dose of [^{14}C]giredestrant capsule, 30.8 mg [^{14}C]giredestrant containing 3.88 MBq (105 µCi) ^{14}C, with approximately 240 mL water following a minimum 10 hour fast. Urine, feces, and blood samples were collected predose and at predefined intervals throughout the study period. Safety and tolerability were monitored throughout the study and participants remained in the clinic until Day 21. The subjects returned for a total of 3 outpatient visits every 7 days for a 24-hour sample collection interval prior to study completion, i.e., on Days 28, 35 and 42.

Part 2 was intended to evaluate the absolute bioavailability and relative bioavailability of two oral formulations of giredestrant indicated here as Formulation12 and Formulation18. Each subject received each of the following treatments: 30 mg of giredestrant in 10 mL as an intravenous infusion over 30 minutes (min; Treatment B), 30 mg Formulation12 capsule administered orally with 240 mL water (Treatment C), and 30 mg Formulation18 capsule administered orally with approximately 240 mL water (Treatment D). Subjects were randomly allocated to one of two treatment sequences: B-C-D and B-D-C in an open-label design. There was a washout period of at least 10 days between each treatment. Subjects were admitted in the morning on the day prior to the first giredestrant administration and resided in the clinical unit until Day 8 in Period 3. In each treatment, participants received a single dose of giredestrant after a minimum of 10 hours fasting. Blood samples for measurement of plasma giredestrant were collected predose and at intervals until Day 8 of each treatment period; safety and tolerability were monitored throughout the study. Formulation18 will be advanced in

DMD Fast Forward. Published on June 4, 2024 as DOI: 10.1124/dmd.124.001688
This article has not been copyedited and formatted. The final version may differ from this version.

clinical development and only the results of the absolute bioavailability (aBA) of this formulation are reported herein.

Safety assessments and analyses in both Parts 1 and 2, consisted of monitoring and recording adverse events (AEs), including serious AEs (SAEs) and AEs of special interest, performing safety laboratory assessments, measuring vital signs, and conducting other tests (including ECGs and physical examinations). All participants who received at least one dose of IMP were included in the safety analyses.

Subjects:

The study enrolled six (Part 1) and ten (Part 2) healthy WNCBP who were non-pregnant, non-lactating and who were either postmenopausal or surgically sterile, aged 30 to 65 years, with a body mass index between 18.5 and 32.0 kg/m^2 and regular bowel movements (Part 1 only). All subjects provided written informed consent before study screening. Participants were screened for inclusion up to 28 days prior to the first dose of study drug.

Women of childbearing potential were excluded from the trial because the anti-estrogenic activity of giredestrant may cause adverse effects in pregnancy and pose a risk to the human fetus. Men were excluded because there was no clinical safety or pharmacokinetic (PK) data on giredestrant administration in males at the time of study initiation. A dose of 30 mg was used as this is the anticipated clinical dose for giredestrant in the treatment of breast cancer.

DMD Fast Forward. Published on June 4, 2024 as DOI: 10.1124/dmd.124.001688
This article has not been copyedited and formatted. The final version may differ from this version.

In addition to routine Phase 1 study exclusion criteria, participants were excluded if any of the following criteria were applicable. For Part 1 only: exposure to significant radiation (exceeding 5 millisievert (mSv) in the last 12 months or 10 mSv in the last 5 years), history of GI surgery (with the exception of appendectomy unless it was performed within the previous 12 months); acute diarrhea or constipation in the 7 days before the predicted Day 1. For both Parts: use of prescription medication within 2 weeks prior to giredestrant administration, use of oral antibiotics within 4 weeks or IV antibiotics within 8 weeks prior to admission, malabsorption syndrome or other condition that can interfere with enteral absorption, current severe acute respiratory syndrome coronavirus 2, or administration of any investigational medicinal product within 90 days of Day 1. Participants who took part in Part 1 of the clinical trial were unable to join Part 2.

Dose rationale:

Giredestrant has been shown to be safe, well-tolerated and exhibits dose proportional increases in PK exposure, at doses from 10 mg to 250 mg once daily (QD) and the 30 mg dose was selected for further evaluation in Phase II/III trials (Malhi et al., 2023). Therefore, a dose of 30 mg was considered suitable to acquire mass balance and aBA data.

The dose of radioactivity was determined following review of nonclinical quantitative whole body autoradiography data and the consequent human dosimetry prediction. The effective dose was 0.7 mSv and fell within International Commission on Radiological Protection (1992) Guidelines for Category IIa studies (0.1 to 1 mSv). The dose of

DMD Fast Forward. Published on June 4, 2024 as DOI: 10.1124/dmd.124.001688
This article has not been copyedited and formatted. The final version may differ from this version.

radioactivity was not more than 4.6 MBq (124 μCi) with the actual dose to each subject being 30.8 mg, 105 μCi.

Sample collection and preparation:

Part 1: Blood and plasma samples for PK analysis of giredestrant, TR, and metabolite profiling and identification were collected predose and 1, 1.5, 2, 2.5, 3, 4, 5, 6, 8, 12, 24 hours postdose and every 24 hours thereafter until Day 21. Urine samples for TR measurement and metabolite profiling were collected predose, at 0-12 and 12-24 hours postdose, and then at 24-hour intervals until Day 21. Blood and plasma samples for PK analysis of giredestrant and TR were collected during return visits on Day 28, 35 and 42 postdose; urine samples were also collected for a 24-hour interval during these visits.

For each period, all urine produced by a subject was collected into individual 500 mL polypropylene/polyethylene containers and refrigerated. At the end of the collection period, the bulk urine was mixed thoroughly, the total weight recorded, and aliquots transferred to polypropylene containers and stored frozen at approximately 80℃ until analysis and/or sample pooling.

Fecal samples were collected at predose and 24-hour intervals until Day 21. Fecal samples were also collected for a 24-hour interval during return visits on Day 28, 35 and 42 postdose. Each fecal collection was transferred to a tared container and homogenized with approximately 2 to 3 volumes of water and the weight of the fecal homogenate was recorded. For each collection interval, 0.2 – 0.5 g of each fecal homogenate sample was combusted using an automatic sample oxidizer prior to measurement of radioactivity. The remaining bulk fecal homogenate samples were

DMD Fast Forward. Published on June 4, 2024 as DOI: 10.1124/dmd.124.001688
This article has not been copyedited and formatted. The final version may differ from this version.

stored at approximately 80℃ until used for preparing pooled samples for biotransformation analysis.

Part 2: Plasma samples for the measurement of giredestrant were taken predose, 1, 1.5, 2, 3, 4, 6, 8, 12, 24, 48, 72, 96, 120, 144 and 168 hours postdose (relative to start of infusion for IV dose) for both IV and oral administration. Plasma samples were additionally taken at 0.25, 0.5, 0.58, 0.67 hours postdose after IV administration and 2.5 and 5 hours post oral administration.

Study drugs, reference compounds and chemicals:

For Part 1 of the trial, [^{14}C]giredestrant was supplied by Pharmaron UK Ltd (Rushden, Northamptonshire, UK) as a white to yellow powder (Batch number: RLM 205) with specific activity of 3.41 µCi/mg (free base) and a radiochemical assay purity of >99.9%. The chemical structure of giredestrant is shown in **Figure 5** and the position of the radiocarbon is indicated by an asterisk. The drug capsules were manufactured as Swedish orange, size 3 Hypromellose capsules by Quotient (Nottingham NG11 6JS, UK) (Batch number: 204283/C/01).

For Part 2 of the trial, the active pharmaceutical ingredient of the giredestrant Solution for Infusion was supplied by Roche as a white powder (Batch number: BS1909SA01). A Solution for Infusion (Treatment B) was manufactured as a clear, colorless to pale yellow solution (3 mg/mL giredestrant) by Quotient (Batch numbers 204283/C/02 and 204283/C/05). Formulation18 capsules (Treatment D) were hard capsules of 30 mg giredestrant manufactured as a dark-green, size 3 HPMC capsule by Roche (Batch number 1167113 and 1167266, respectively). Both [^{14}C]giredestrant and giredestrant

DMD Fast Forward. Published on June 4, 2024 as DOI: 10.1124/dmd.124.001688
This article has not been copyedited and formatted. The final version may differ from this version.

doses are expressed as the free base equivalent in Part 1 and 2. Only the data for the clinical Formulation18 are reported in this study.

Acetic acid was purchased from Fisher Scientific (Fair Lawn, NJ). Acetonitrile (ACN) and Ultrapure high-performance liquid chromatography (HPLC) grade water were from EMD Millipore Corporation (Billerica, MA). Ammonium acetate was purchased from Sigma-Aldrich (St. Louis, MO). Pico-Fluor 40 Carbon-14 cocktail for liquid scintillation counting (LSC) was purchased from Perkin Elmer (Waltham, MA). All other chemicals were of reagent grade or HPLC grade and obtained from commercial suppliers.

Determination of unlabeled giredestrant plasma concentrations:

Giredestrant plasma concentrations were determined at Covance Laboratories, Inc. (Madison, WI) using a validated liquid chromatography (LC)-tandem mass spectrometry (MS/MS) method. Giredestrant and its internal standard [^{13}C8, ^{15}N]-giredestrant were extracted from human plasma by supported liquid extraction. LC-MS/MS analysis was carried out on a Shimadzu LC-30AD system (Kyoto, Japan) coupled to a Sciex API 5500 triple quadrupole mass spectrometer (Framingham, MA, US). The mass spectrometer was operated in positive electrospray ionization (ESI) mode under optimized conditions with Multiple Reaction Monitoring (MRM) of analytes and the internal standard (Giredestrant concentrations were calculated with the use of a standard curve with a 1/x2 linear regression over a concentration range of 1 to 1000 ng/mL or 0.1 to 100 ng/mL. The precision and accuracy of assays were satisfactory throughout the study. The lower limit of quantification (LLOQ) was 1 ng/mL.

Determination of radioactivity:

DMD Fast Forward. Published on June 4, 2024 as DOI: 10.1124/dmd.124.001688
This article has not been copyedited and formatted. The final version may differ from this version.

TR in plasma, urine, and feces was determined at Pharmaron UK Ltd, (Rushden, Northamptonshire, UK) by liquid scintillation counting. Radioactivity in fecal homogenate and whole blood was determined after combustion in oxygen using an Automatic Sample Oxidiser (Model 307, Perkin Elmer (formerly Packard)). The combustion products (CO_2) were absorbed into Carbon Trap (Meridian Biotechnologies Ltd.) and mixed with the scintillation cocktail Carbon Count (Meridian Biotechnologies Ltd.) for measurement of radioactivity by LSC. The efficiency of the oxidizer was checked at regular intervals (approximately every 24 samples) using carbon-14 standards and was ≥96%. Radioactivity in urine, plasma and dose vessel rinses was quantified directly. Samples were mixed with Gold Star scintillation fluid (Meridian Biotechnologies Ltd., ratio of scintillant: sample ranged between ca. 2:1 and ca. 7:1) and counted by LSC. The lower limits of detection for plasma, whole blood, and urine were 11.4 ng equivalents (eq) (free drug)/mL, 10.4 ng eq (free drug)/mL and 0.42 ng eq (free drug)/g, respectively.

Extraction of metabolites from biological samples:

Plasma samples at predose and 1, 1.5, 2, 2.5, 3, 4, 6, 8, 12, 24, and 48 h (Subjects 101, 104 and 106); 72 h (Subjects 102 and 105); and 96 h (Subject 103) postdose were

DMD Fast Forward. Published on June 4, 2024 as DOI: 10.1124/dmd.124.001688
This article has not been copyedited and formatted. The final version may differ from this version.

pooled proportionally to the PK area under the curve (AUC) (Hop et al., 1998). Approximately 6 mL of ACN was added to 2 mL of pooled plasma (3:1, volume to volume [v/v]), and the mixture was vortexed for 5 min at room temperature. The samples were centrifuged at 3000 rpm for 10 min at room temperature and the supernatant was transferred to a new set of tubes. The plasma pellet was re- suspended in 0.5 mL of water and the same extraction procedures were repeated twice. The supernatants from three extractions were combined, evaporated to approximately 130 µL, and added to 20 µL of ACN to mix. The mixture was centrifuged under 18000 x *g* for 6 min and the supernatant was injected for LC-MS radioprofile analysis.

Time-pooled urine and feces samples were prepared for each subject by mixing an equal percentage of the excreted volume or weight of each collection. Each pooled urine and feces sample for metabolite profiling represented greater than 68% and 88% of the TR excreted in that matrix, respectively. Each pooled urine sample (5 mL) was extracted and concentrated using a 6 cc Oasis Cartridge (Water; Milford, MA; Part No 18603379). The cartridge was washed with 5 mL of methanol followed by 7 mL of water to equilibrate the cartridge. A 5 mL urine sample was loaded on the cartridge and eluted with 7 mL of methanol. The samples were concentrated down using a SpeedVac™ concentrator to approximately 100 µL and a 1:3 ACN-to-water solution (100 µL) was added into the concentrated urine sample. After mixing the sample, it was centrifuged at 18000 x *g* for 6 min to remove undissolved solids. The supernatant was directly injected for LC- MS radioprofile analysis.

DMD Fast Forward. Published on June 4, 2024 as DOI: 10.1124/dmd.124.001688
This article has not been copyedited and formatted. The final version may differ from this version.

Approximately 1 gram of pooled fecal homogenate from each subject was used for extraction by adding 1 mL of water, followed by 5 min vortex, and then adding 3 volumes of ACN (3:1, volume per weight [v/w]). The mixture was then vortexed for 5 min and sonicated for 5 min at room temperature. The samples were centrifuged at 3000 rpm for 10 min and the supernatant was transferred to a new set of tubes. The post- extraction solids were then resuspended into one volume of water and the extraction procedures were repeated twice. The supernatants from three extractions were evaporated using a SpeedVac^{TM} to approximately 1 mL and they were centrifuged at 3000 rpm for 10 min. The three supernatants were combined and transferred to a new glass tube. The combined supernatant was dried using SpeedVac^{TM} to about 1 mL. Each original tube was washed with 1 mL of ACN and centrifuged at 3000 rpm for 10 min. The supernatants were combined and transferred to a new glass tube and dried to approximately 1 mL. The supernatant of the washing solution was combined with the first supernatant solution. The mixture was dried down to 800 µL and followed by addition of 200 µL ACN and 30 µL DMSO. The sample was vortexed and then centrifuged at 3000 rpm for 10 min before it was injected (50-100 µL) onto LC/MS for radioprofile analysis.

Metabolite profiling and identification:

Chromatographic separations were completed using a Nexera X2 LC system (Shimadzu, Kyoto, Japan) and a Nexera X2 SIL-30 AC MP autosampler (Shimadzu, Kyoto, Japan) using a Luna Omega polar C18 column (3 micron, 4.6 x 150 mm, Phenomenex) and mobile phases A (20 mM ammonium acetate in water and adjusted to pH 8 with ammonium hydroxide) and B (20 mM ammonium acetate in ACN (90) :

DMD Fast Forward. Published on June 4, 2024 as DOI: 10.1124/dmd.124.001688
This article has not been copyedited and formatted. The final version may differ from this version.

water (10)). For the gradient, the initial conditions were 17% B for 2 min, increased to 65% B over 30.5 min, increased to 95% B over 0.5 min and maintained for 2 min for column flushing, then returned to 17% B over 0.1 min, and re-equilibrated to these conditions for 9 min. The total run time was 44 min. For detection, the flow from the column was split 10:1 with the minor component directed to the mass spectrometer and the major component directed to a fraction collector for collection to DeepWell LumaPlate 96-well plates (Perkin Elmer, Waltham, MA) based on time (10 seconds/fraction). Following fraction collection, the plates were dried under vacuum using a SpeedVac^{TM} (Labconco) with low or medium heat setting for up to 8 hours, then the plate was sealed with transparent TopSeal cover (PerkinElmer, Shelton, CT). The radioactivity in each fraction was measured using a TopCount Scintillation and Luminescence Counter (Perkin Elmer) for 5 min. Radiochromatograms were reconstructed using Laura Evaluation software (LabLogic, Sheffield, United Kingdom) and all radiopeaks that were discernible over background (signal at least 3) were integrated to determine the distribution of radioactivity in each sample.

The proposed metabolite structures were determined from MS/MS data that corresponded to the radiodetection of drug-related analytes. Mass spectra were obtained with an Orbitrap Fusion Lumos high-resolution mass spectrometer equipped with an electrospray ionization source from Thermo Scientific. The electrospray ion source voltage was 3.0 kV. The heated capillary temperature was 300^0C. The scan-event cycle consisted of a full-scan mass spectrum at a mass resolving power of 60,000 and the corresponding data-dependent MS/MS and MS^n scans were acquired at a

DMD Fast Forward. Published on June 4, 2024 as DOI: 10.1124/dmd.124.001688
This article has not been copyedited and formatted. The final version may differ from this version.

resolving power of 15,000. Accurate mass measurements were performed using external calibration.

Pharmacokinetic evaluation and data analysis:

Mass balance parameters were calculated for TR in urine and feces separately and combined. For each collection interval, the amount excreted in each matrix (i.e., urine (Ae(urine)) and feces (Ae(feces)) was calculated as:

$$Ae(< matrix >) = concentration * weight$$

The total amount excreted in urine and feces combined (Ae(total)), was calculated as:

$$Ae(total) = Ae(urine) + Ae(feces)$$

The cumulative amount excreted in each matrix (CumAe(urine), CumAe(feces)) was calculated by the incremental summation of the Ae(<matrix>) across all collection intervals. The cumulative amount excreted in both urine and feces combined (CumAe(total)) was calculated as:

$$CumAe(total) = CumAe(urine) + CumAe(feces)$$

The % of the TR excreted in each matrix (Fe(urine), Fe(feces)) was calculated for each collection interval as:

$$Fe(< matrix >) = 100 * \frac{Ae(< matrix >)}{Total\ Radioactive\ Dose\ Administered}$$

The combined % of the TR dose excreted in urine and feces was calculated as:

$$Fe(total) = Fe(urine) + Fe(feces)$$

DMD Fast Forward. Published on June 4, 2024 as DOI: 10.1124/dmd.124.001688
This article has not been copyedited and formatted. The final version may differ from this version.

The cumulative % amount of the TR dose excreted was calculated by the incremental summation of the Fe(<matrix>) across all collection intervals and the combined cumulative % was calculated as:

$$CumFe(total) = CumFe(urine) + CumFe(feces)$$

Following Day 21, where urine/fecal collections are no longer continuous and spot sampling days (i.e., 24 h) commenced, additional interpolation of Ae was performed to estimate amount excreted on non-collection days (i.e., over the entire interpolation interval), as follows:

$$Ae(interval) = (\frac{Ae\ 24h[Day\ x + Day\ y]}{2}) * duration\ of\ interval\ (days)$$

where Day x and Day y are the actual amounts excreted for the preceding and proceeding days of the interpolation interval and the interval is considered to be from Day X+1 to Day Y-1.

PK parameters were estimated where possible and appropriate for each subject profile by non-compartmental analysis methods using Phoenix WinNonlin software (Version 8.0 or a more recent version, Certara USA, Inc., USA) for giredestrant in plasma (Parts 1 and 2), and TR in plasma and whole blood (Part 1 only). Actual blood sampling times were used (and actual time relative to start of infusion for IV dose) in the PK analysis. Predose sample times and values that were below the limit of quantitation (BLQ) obtained prior to C_{max} were entered as zero and values that were BLQ after C_{max} were treated as missing. The calculation method for the AUC parameters was linear trapezoidal when concentrations were increasing and log trapezoidal when concentrations were decreasing (linear up-log down method in WinNonlin). At least 3

DMD Fast Forward. Published on June 4, 2024 as DOI: 10.1124/dmd.124.001688
This article has not been copyedited and formatted. The final version may differ from this version.

points, not including C_{max} were required for lambda-z estimation, and at least 3 consecutive measurable concentrations were required to calculate an AUC. The ratio of plasma giredestrant AUC from time 0 to 72 hours ($AUC_{0–72}$) over TR $AUC_{0–72}$ was calculated. Blood to plasma ratios for TR were calculated as:

$$BP\ Ratio = \frac{AUC_{0-72}\ TR\ whole\ blood}{AUC_{0-72}\ TR\ plasma}$$

The ratios were also calculated with AUC from time 0 to the last measurable concentration ($AUC_{0\text{-last}}$).

Statistical analysis

No formal statistical analysis was carried out on Part 1 data. In Part 2, to evaluate the absolute bioavailability of the Formulation18 capsules, log-transformed $AUC_{0\text{-inf}}$ was analyzed using mixed effect modeling techniques. The model included terms for treatment and sequence fitted as fixed effects and subject nested within sequence as a random effect. The mean, including difference from the comparison and the associated 90% confidence interval (CI) obtained from the model were back transformed from the log scale to obtain adjusted geometric mean, adjusted geometric mean ratio (GMR) and 90% CI of the ratio. The statistical analysis was performed using actual treatment. The model was fitted using the SAS Software procedure PROC MIXED.

***In vitro* P450 inhibition study in hepatocytes**

In the *in vitro* experimental conditions, giredestrant (1 µM) was incubated with human hepatocytes (0.5 x 10^6 cells/mL), in the presence and absence of inhibitors. The inhibitors were 1-aminobenzotriazole (ABT at 1 mM with pre-incubation for 30 min) and

DMD Fast Forward. Published on June 4, 2024 as DOI: 10.1124/dmd.124.001688
This article has not been copyedited and formatted. The final version may differ from this version.

tienilic acid (10 μM) which were used together to broadly inhibit P450 activity. The monitoring of metabolites M3, M6 and M8 was undertaken and the corresponding results are tabulated in **Table S3**.

Rat mass balance study

Female Sprague Dawley rats were administered a single oral dose of 30 mg/kg of [^{14}C]giredestrant (200 μCi/kg) (Group 1). Additionally, a group with bile-duct cannulation (BDC) was evaluated for biliary excretion (Group 2). To facilitate collection of specimens, the animals were housed in metabolic cages. The specimens collected included urine, feces, plasma, and biliary samples. The analysis and profiling of these samples was carried out using similar processes and techniques as those utilized for human subjects described above.

DMD Fast Forward. Published on June 4, 2024 as DOI: 10.1124/dmd.124.001688
This article has not been copyedited and formatted. The final version may differ from this version.

Results

Subjects

Six WNCBP were enrolled in Part 1 and ten WNCBP were enrolled in Part 2. The subjects were non-smokers and in good health as judged by pre-established criteria from the investigators. The mean (range) age, weight, and body mass index of the subjects in Part 1 of the study were 56 (50 - 60) years, 75.1 (57.8 - 85.2) kg and 27.8 (23.2 - 30.7) kg/m^2, respectively. The mean (range) age, weight, and body mass index of the subjects in Part 2 of the study were 58 (52 - 65) years, 72.2 (49.5-101.0) kg and 26.8 (20.1 - 31.5) kg/m^2, respectively. All subjects were white and none were Hispanic or Latino. All enrolled subjects in both Part 1 and Part 2 completed the study in accordance with the protocol.

Mass balance

The mean cumulative recovery of radioactivity from the six subjects is shown graphically in **Figure 1**. During the 42-day collection period, the estimated mean total recovery of giredestrant-related radioactivity was 77.0% (range 74.2 - 80.5%) of the administered oral dose of [^{14}C]giredestrant. The majority of the administered radioactivity (68%) was recovered in the feces, with approximately 6.45% recovered in the first 48 hours post- dose (**Table S1**). The radioactivity excreted in urine was low throughout the study duration and cumulatively accounted for 9.04% of the administered radioactive dose.

DMD Fast Forward. Published on June 4, 2024 as DOI: 10.1124/dmd.124.001688
This article has not been copyedited and formatted. The final version may differ from this version.

PK of TR and unlabeled giredestrant

The mean plasma concentration-time profiles for giredestrant and TR following a single oral dose of 30.8 mg [^{14}C]giredestrant are shown in **Figure 2** and the associated PK parameters are summarized in **Table 1**.

Giredestrant and TR in plasma and whole blood were observed at the first PK time point of 1-hour postdose in all 6 subjects. The median (range) T_{max} was 3.5 hours (2.00 - 5.00 hours), 5.00 hours (2.00 - 5.00 hours) and 5.00 hours (2.5 - 5.00 hours) postdose, for giredestrant in plasma, TR in plasma, and TR in whole blood, respectively. While the median TR T_{max} seems delayed with respect to giredestrant, note that there are multiple peaks in the PK profiles and the range of T_{max} is comparable. Mean C_{max} values were 74.3 ng/mL, 124 ng eq (free drug)/mL, and 88.0 ng eq (free drug)/mL for giredestrant in plasma, TR in plasma, and TR in whole blood, respectively. Concentrations subsequently declined in a biphasic manner for all 3 analytes with mean elimination half-lives of 42.6 hours, 48.4 hours, and 50.8 hours, respectively. Terminal slopes were reliably determined for 3 out of 6 subjects for whole blood TR and $AUC_{0\text{-}inf}$ was reliably determined for 3 of 6 subjects for both plasma and whole blood TR. Intersubject variability in the PK parameters was low to moderate (20.6% to 40.8%).

The geometric mean (geometric CV%) plasma $AUC_{0\text{-}t}$ ratio for giredestrant to TR was 0.625 (12.7%), indicating that giredestrant was the main circulating species in plasma. The geometric mean (geometric CV%) whole blood to plasma TR concentration ratios ranged from 0.672 (2.8%) to 1.02 (27.5%), indicating no notable preferential distribution

DMD Fast Forward. Published on June 4, 2024 as DOI: 10.1124/dmd.124.001688
This article has not been copyedited and formatted. The final version may differ from this version.

of TR to the cellular components of whole blood. There were also no notable time-dependent differences in the ratios.

Absolute bioavailability of giredestrant

The mean plasma giredestrant concentration versus time profiles following IV (30 mg, 30 min infusion) and oral (30 mg Formulation18 capsule) administration of giredestrant are presented in **Figure 3**. Corresponding plasma PK parameters are summarized in **Table 2**.

Maximum plasma concentrations of giredestrant occurred between 0.25 and 0.60 hours postdose following a single IV infusion of 30 mg giredestrant solution over 30 min. Concentrations then declined in a biphasic manner and remained quantifiable until the last sampling time point of 168 hours postdose. Terminal slopes were reliably determined for all 10 subjects and resulted in a geometric mean (geometric CV%) half-life of 37.8 (33.9%) hours. Following the IV dose, giredestrant had a plasma clearance and volume of distribution of 5.31 L/h and 266 L, respectively.

Following a single oral dose of a 30 mg Formulation18 capsule, plasma concentrations of giredestrant were evident from the first sampling time point of 1-hour postdose in all subjects. One subject was excluded from the PK analysis set because the subject had quantifiable predose concentrations of giredestrant that were >5% of C_{max}. Maximum plasma concentrations occurred between 2 and 5 hours postdose. Concentrations then declined in a biphasic manner and remained quantifiable until between 144 hours postdose and the last sampling time point of 168 hours postdose. Terminal slopes were reliably determined for all 9 subjects and resulted in a geometric CV% half-life of 36.4

DMD Fast Forward. Published on June 4, 2024 as DOI: 10.1124/dmd.124.001688
This article has not been copyedited and formatted. The final version may differ from this version.

hours. The absolute bioavailability (90% CI) of giredestrant following oral administration of a 30 mg Formulation18 capsule, as measured by $AUC_{0\text{-}inf}$, was 58.7% (54.0, 63.8) (**Table S2**)

Metabolite profiling and identification in plasma and excreta

The extraction recoveries ranged from 90.8% to 98.1% for the pooled plasma samples and from 85.0% to 94.5% for urine samples. The extraction recoveries of fecal homogenate were greater than 75% for all subjects except one, for whom recovery was 64.7%.

Representative radiochromatograms of pooled plasma, urine, and fecal samples from an individual subject are presented in **Figure 4**.

The relative abundances and exposures of giredestrant and its metabolites in plasma and their percentage of dose detected in urine and feces are presented in **Table 3**. In pooled human plasma, giredestrant represented the major drug-related component (56.8% of the total drug-related plasma AUC exposure). The direct glucuronide M3 was the major circulating metabolite in circulation, accounting for 10.2% of the total drug-related exposure. Several other metabolites were detected, with each accounting for less than 10% of the total drug-related exposure including M1 (hydroxylation + glucuronidation), M18 (hydroxylation), M12 (epimerization), M22 (hydroxylation) and M25 (dehydrogenation).

Pooled urine and feces samples from each subject were also analyzed for metabolite profiles. In urine, giredestrant accounted for 1.90% of the total dose. The most abundant

DMD Fast Forward. Published on June 4, 2024 as DOI: 10.1124/dmd.124.001688
This article has not been copyedited and formatted. The final version may differ from this version.

urinary metabolite was M3 (glucuronidation), representing 2.09% of the total dose and all other metabolites were at trace levels (<1.1% of the dose). In feces, giredestrant and the sum of all metabolites accounted for 20.0% and 44.7% of the dose, respectively. All identified metabolites in feces were formed as a result of oxidative metabolism, none of which accounted for more than 10% of the total dose (**Table 3**). No glucuronide metabolites (including M3, the most abundant metabolite in plasma) were detected in feces indicating that these conjugated metabolites were likely cleaved during gastrointestinal transit.

In total, twenty metabolites were identified in the current study in either plasma, urine, and/or feces. The proposed structures of these metabolites were derived from elemental compositions calculated based on the accurate masses and product ion spectra. The proposed metabolic pathways for giredestrant in humans are summarized in **Figure 5**.

The molecular ion $[M + H]^+$ and major product ions observed by high resolution full scan and MS^2 experiments for giredestrant and its metabolites are listed in **Table 4** and the metabolites structures elucidations are summarized in **Figures S1 - S21**.

In vitro P450 inhibition study in hepatocytes

In human hepatocytes, GDC-9545 was susceptible to metabolism, with 33.5% remaining after 180 minutes. This depletion was not appreciably reduced by ABT (a broad spectrum CYP inhibitor that inhibits the major CYP isoforms, except CYP2C9) and tienilic acid (a selective inhibitor of CYP2C9). Formation of M3 (glucuronide) was not appreciably inhibited (11% inhibition) by ABT and tienilic acid, whereas formation of

DMD Fast Forward. Published on June 4, 2024 as DOI: 10.1124/dmd.124.001688
This article has not been copyedited and formatted. The final version may differ from this version.

M6 (N-dealkylation) and M8 (N-dealkylation) were completely inhibited by these inhibitors.

Rat mass balance study

Following a single oral dose of 30 mg/kg [^{14}C]giredestrant to female intact rats, giredestrant constituted the majority of plasma content (96.4%). Fecal excretion was the major route of elimination and accounted for 90.9% of the total radioactivity (**Table S4, Figure S22**). Giredestrant accounted for 47.4% of the administered dose in feces. Ten metabolites accounted for less than 7.24% of the administered dose, including M4 (N-dealkylation) and M9 (hydroxylation) as the most abundant metabolites (**Table S4, Figure S22**). Urinary excretion was minimal (1.72%, **Table S5, Figure S22**).

In BDC rats, biliary excretion made up 38.9% of the administered dose (**Table S6, Figure S22**), with the major constituent being M3 (glucuronidation) at 16.7% of administered dose. Overall, the major metabolic pathways for giredestrant involved glucuronidation (M2, M3), oxidation, sulfonation, hydroxylation, dehydrogenation, N-dealkylation, hydrogenation + sulfonation, hydration + sulfonation, oxidative defluorination, and epimerization (**Table S4, Figure S23**).

Safety and tolerability

Overall, single oral and IV doses of 30 mg giredestrant were well tolerated with no deaths, no SAEs or severe (NCI CTCAE Grade ≥3) AEs, no AEs of special interest (AESIs), and no subject withdrawn from the study as a result of an AE. In Part 1, all

DMD Fast Forward. Published on June 4, 2024 as DOI: 10.1124/dmd.124.001688
This article has not been copyedited and formatted. The final version may differ from this version.

reported AEs were mild (NCI CTCAE Grade 1), and none were considered to be related to giredestrant by the investigator. All AEs resolved by the end of the study without sequelae. In Part 2, all reported AEs were mild (NCI CTCAE Grade 1) or moderate (NCI CTCAE Grade 2) in maximum severity. Three out of 10 subjects reported 3 AEs considered related to giredestrant by the investigator (1 out of 10 subjects reported 1 event each following administration of giredestrant as solution for infusion and as Formulation18 capsule). These events comprised night sweats, fatigue (both mild [NCI CTCAE Grade 1]), and headache (moderate [NIC CTCAE Grade 2]). There were no notable differences in the safety profiles for any treatment (i.e., either IV solution for infusion or oral capsules). All AEs resolved by the end of the study without sequelae. Additionally, there were no clinically significant individual changes from baseline in safety laboratory parameters, vital sign, or ECG results during the study.

DMD Fast Forward. Published on June 4, 2024 as DOI: 10.1124/dmd.124.001688
This article has not been copyedited and formatted. The final version may differ from this version.

Discussion

After oral administration of [^{14}C]giredestrant to healthy subjects, the average total estimated excretion of radioactivity was 77% of the administered dose over an excreta collection period of 42 days, with most giredestrant-related radioactivity eliminated in feces (68%) and a small amount in urine (9%) (**Figure 1 and Table S1**). Although the overall recovery of giredestrant was sufficient to elucidate its major clearance pathways as well as the identification of its major metabolites, there was a longer retention in plasma and lower dose recovery in excreta than expected. Several reasons for these characteristics are possible. Measurable radioactivity was recovered in excreta for each of the 6 subjects at Day 42, indicating that more complete recovery could be achieved by collection over a longer duration. Partially, losses could be introduced by the estimation (interpolation) method that used samples from single weekly 24-hour collections to estimate recovery over 3 weeks after patients were discharged from the clinic on Day 21. Importantly, enterohepatic recirculation (EHR) and possibly intestinal re-absorption (IR), as discussed later, could be a contributing factor for the long retention and low recovery of giredestrant.

Metabolite profiling results indicated extensive metabolism of giredestrant with only 22% of the administered radioactivity excreted as parent drug (feces 20.0% and urine 1.90%). Limited recovery in urine is consistent with the previously reported results in patients with breast cancer (Malhi et al., 2023). A direct glucuronide of giredestrant, M3, was the major circulating metabolite. There were 5 minor circulating metabolites which were products of hydroxylation, dehydrogenation, or epimerization, with each accounting for less than 10% of the total drug-related exposure. The major circulating

DMD Fast Forward. Published on June 4, 2024 as DOI: 10.1124/dmd.124.001688
This article has not been copyedited and formatted. The final version may differ from this version.

metabolite M3 was also observed in human hepatocyte incubations and in rat bile (**Table S3 and S4**). Based on the following observations with mass spectrometry (MS and MS2) experiments, M3 was assigned as a 0-glucuronide: (1) Fragment m/z 314 of M3 undoubtedly determined that the glucuronidation occurred in the region containing a primary alcohol and a tertiary nitrogen (**Figue S4**). (2) M3 was observed as a major metabolite in rat bile (**Table S4**). (3) It is known in the literature that quaternary N(+)-glucuronide may not occur or only be at trace level in rats (Lee Chiu and Huskey, 1998, Zhang et al, 2023).

M3 was also detected in human urine. Interestingly, the majority of dose was recovered as oxidative metabolites in humans and no glucuronides were observed in feces (**Table 3**). In feces, a total of 12 oxidative metabolites (2-5% of the dose) were identified, collectively accounting for approximately 45% of the administered dose, which suggested a potentially significant role of CYP-mediated metabolism in humans. Conversely, when employing *in vitro* hepatocyte models along with a broad-ranging CYP inhibitor, 1-aminobenzotriazole (ABT), the assessments of CYP metabolism revealed only a limited involvement of CYP-mediated metabolic processes (**Table S3**). We hypothesize this *in vitro - in vivo* difference is due to EHR and/or IR, where the low clearance in humans could potentially elevate the role of CYP-mediated metabolism as a crucial pathway for giredestrant elimination. This essentially means that through numerous cycles of excretion and reabsorption, the direct glucuronide is excreted into the intestine, de-conjugated, and reabsorbed efficiently, thereby reducing the glucuronide's apparent contribution to the total clearance. This overall outcome would accentuate the role of oxidative metabolism in the clearance pathway of giredestrant. These observations are consistent with the rat mass balance data where M3 was the

DMD Fast Forward. Published on June 4, 2024 as DOI: 10.1124/dmd.124.001688
This article has not been copyedited and formatted. The final version may differ from this version.

major metabolite in the bile of bile duct cannulated rats, but no M3 was detected in rat feces (**Figure S23**). In the present study, the secondary peak in the giredestrant plasma PK profile at 4-8 h post dose (**Figure 2 inset**) is characteristic of drugs undergoing EHR and is supportive of EHR for giredestrant (Roberts et al., 2002). Evidence from the literature corroborates the suggested mechanism of EHR (Liang et al., 2021; Ganti et al., 2023; Zhang et al., 2021).

Based on the plasma AUC_{0-t} ratio of giredestrant to TR of 0.625, the majority of circulating material in humans was giredestrant. Metabolite identification analyses confirmed that unchanged giredestrant was the most prominent drug-related analyte in pooled plasma, representing 56.8% of the total exposure. The PK profiles of giredestrant in plasma and TR in blood and plasma were similar with comparable half-lives, indicating no metabolites with a long half-life remain in circulation. The parallel terminal phase profiles of parent and TR indicate formation-rate limited PK of the ^{14}C metabolites.

The results of the aBA study (Part 2) demonstrated that giredestrant has low systemic clearance and high volume of distribution (**Table 2**). The low clearance of giredestrant was expected from *in vitro* stability data in hepatocytes and liver microsomes as well as preclinical data (Liang et al., 2021; Ganti et al., 2023). The high volume of distribution relative to total body water volume was consistent with its physicochemical properties and indicates significant distribution to tissues. It has been reported that EHR may decrease clearance and correlate with a larger volume of distribution (Zhang et al 2021; Ibarra et al. 2021). The parallel terminal concentration−time profiles after oral and IV

DMD Fast Forward. Published on June 4, 2024 as DOI: 10.1124/dmd.124.001688
This article has not been copyedited and formatted. The final version may differ from this version.

administration of giredestrant (**Figure 3**) were indicative of elimination rate-limited PK.

Overall, the plasma PK profile, the associated plasma PK parameters and the low-moderate interindividual variability for giredestrant in this study were comparable to those observed earlier in patients with ER+ HER2-negative locally advanced/metastatic breast cancer, and in healthy WNCBP (NCT04274075 unpublished data; Malhi et al., 2023).

The fraction absorbed in human (Fa) following oral administration could only be approximated in this study since the radioactivity recovered in feces as parent drug (20.0% of the dose) is likely a combination of unabsorbed giredestrant, biliary excretion of giredestrant, and deconjugated glucuronide metabolites. Indeed, the metabolite identification data (**Table 3**) showed that the circulating glucuronide metabolite M3 was absent in feces, presumably due to beta-glucuronidase activities in the gastrointestinal tract. Therefore, an estimated Fa of 0.54, derived from combining the TR retrieved in urine (9.04%) and the radioactivity identified in feces as metabolites (44.7%), is likely an underprediction of giredestrant's absorption. A range of Fa values (0.64 to 0.94) was therefore proposed to reflect the uncertainty in this PK parameter and was based on the following hypotheses. According to mass balance and metabolite ID data, renal excretion was low (Fe = 0.019) with a corresponding low renal plasma clearance ($CL_{r,p}$) of 0.17 L/h ($CL_{r,p}$ = (Fe/F) * CL_{IV}). Therefore, hepatic plasma clearance ($CL_{h,p}$) was 5.14 L/h ($CL_{h,p}$ = CL_{IV} - $CL_{r,p}$) and hepatic blood clearance $CL_{h,b}$ was 6.44 L/h ($CL_{h.b}$ = $CL_{h,p}$ / B:P ratio) with B:P = 0.8 from *in vitro* experiments. Accordingly, the fraction escaping hepatic metabolism Fh was estimated to be 0.93 (Fh = 1 - $CL_{h.b}/Q_h$ based on Q_h of 20.7 mL/min/kg or 87 L/hr for a 70 kg person). Since oral bioavailability is a product of Fa, Fg

DMD Fast Forward. Published on June 4, 2024 as DOI: 10.1124/dmd.124.001688
This article has not been copyedited and formatted. The final version may differ from this version.

and Fh, Fa in humans can be estimated to be at least 0.64 based on the assumption that intestinal metabolism is low (Fraction escaping gut metabolism Fg = 1). This calculation does not consider the impact of EHR on CL_{IV} which may bring additional uncertainty. Alternatively, based on the radioactivity recovered in feces during a mean human intestinal transit time of 48 hours (6.45%, **Table S1**), Fa can be estimated to be 0.94 (1 - 0.0645). This method implies that intestinal metabolism may be important (Fg = 0.68). *In vitro* studies to understand the impact of intestinal metabolism are currently ongoing. Total metabolites in urine and feces combined represented 51.0% of the dose. Therefore, the fraction metabolized (Fm) was estimated to range from 0.54 to 0.80 (0.51 / 0.64 or 0.94). A graphical representation of the proposed disposition of giredestrant following a single oral administration to healthy volunteers is summarized in **Figure 6**.

In conclusion, this study comprehensively characterizes the mass balance, elimination routes, metabolic profile, and absolute bioavailability of giredestrant in humans. Orally administered giredestrant was rapidly absorbed, had moderate oral bioavailability, and was extensively metabolized. EHR appeared to play an important role in disposition of giredestrant. Oxidative metabolism followed by excretion in the feces was the major elimination route of giredestrant. Following IV administration, giredestrant exhibited low clearance and moderate volume of distribution in humans.

DMD Fast Forward. Published on June 4, 2024 as DOI: 10.1124/dmd.124.001688
This article has not been copyedited and formatted. The final version may differ from this version.

Acknowledgements

The authors thank the study volunteers, without whom this study would not have been possible. The authors also acknowledge Gina Xiaoxing Wang's scientific input to this work.

Data Availability

Qualified researchers may request access to individual patient level data through the clinical study data request platform (https://vivli.org/). Further details on Roche's criteria for eligible studies are available here (https://vivli.org/members/ourmembers/). For further details on Roche's Global Policy on the Sharing of Clinical Information and how to request access to related clinical study documents, see here (https://www.roche.com/research_and_development/who_we_are_how_we_work/clinical_trials/our_commitment_to_data_sharing.htm).

Authorship Contributions

Participated in research design: Kshirsagar, Chen, Gates, Kawakatsu, Khojasteh, Ma, Musib, Osaghae, Wang, Tang, Zhang, Zhao, De Bruyn

Conducted experiments: Kshirsagar, Chen, Gates, Khojasteh, Ma, Musib, Osaghae, Wang, Cho, Tang, Zhang, Zhao

Contributed new reagents or analytic tools: Ma, Zhang

Performed data analysis: Kshirsagar, Yu, Gates, Khojasteh, Ma, Malhi, Osaghae, Wang, Cho, Tang, Zhang, Zhao, De Bruyn

Wrote or contributed to the writing of the manuscript: Kshirsagar, Chen, Yu, Gates, Kawakatsu, Khojasteh, Ma, Malhi, Osaghae, Wang, Zhang, Zhao, De Bruyn

DMD Fast Forward. Published on June 4, 2024 as DOI: 10.1124/dmd.124.001688
This article has not been copyedited and formatted. The final version may differ from this version.

References

Chandarlapaty S, Chen D, He W, Sung P, Samoila A, You D, Bhatt T, Patel P, Voi M, Gnant M, Hortobagyi G, Baselga J, and Moynahan ME (2016) Prevalence of ESR1 Mutations in Cell-Free DNA and Outcomes in Metastatic Breast Cancer: A Secondary Analysis of the BOLERO-2 Clinical Trial. *JAMA Oncol* **2:**1310-1315.

Fribbens C, O'Leary B, Kilburn L, Hrebien S, Garcia-Murillas I, Beaney M, Cristofanilli M, Andre F, Loi S, Loibl S, Jiang J, Bartlett CH, Koehler M, Dowsett M, Bliss JM, Johnston SR, and Turner NC (2016) Plasma ESR1 Mutations and the Treatment of Estrogen Receptor-Positive Advanced Breast Cancer. *J Clin Oncol* **34:**2961-2968.

Ganti A, Yu S, Sharpnack D, Ingalla E, and De Bruyn T (2023) Physiologically-based pharmacokinetic/pharmacodynamic modeling to predict tumor growth inhibition and the efficacious dose of selective estrogen receptor degraders in humans. *Biopharm Drug Dispos* **44:**301-314.

Guan J, Zhou W, Hafner M, Blake RA, Chalouni C, Chen IP, De Bruyn T, Giltnane JM, Hartman SJ, Heidersbach A, Houtman R, Ingalla E, Kategaya L, Kleinheinz T, Li J, Martin SE, Modrusan Z, Nannini M, Oeh J, Ubhayakar S, Wang X, Wertz IE, Young A, Yu M, Sampath D, Hager JH, Friedman LS, Daemen A, and Metcalfe C (2019) Therapeutic Ligands Antagonize Estrogen Receptor Function by Impairing Its Mobility. *Cell* **178:**949-963 e918.

Hop CE, Wang Z, Chen Q, and Kwei G (1998) Plasma-pooling methods to increase throughput for in vivo pharmacokinetic screening. *J Pharm Sci* **87:**901-903.

Ibarra M, Troconic F, and Fagiolino P (2021) Enteric reabsorption processes and their impact on drug pharmacokinetics. *Scientific Reports* **11:**5794.

Jhaveri KL, Bellet-Ezquerra M, Turner NC, Loi S, Bardia A, Boni V, Sohn J, Neilan TG, Villanueva-Vazquez R, Kabos P, Garcia Estevez L, Lopez-Miranda E, Perez Fidalgo JA, Perez-Garcia JM, Yu J, Fredrickson J, Moore HM, Chang CW, Bond JW, Eng-Wong J, Gates MR, and Lim E (2023) Phase Ia/b Study of Giredestrant +/-Palbociclib and +/-Luteinizing Hormone-releasing Hormone Agonists in Estrogen Receptor-positive, HER2-negative, Locally Advanced/Metastatic Breast Cancer. *Clin Cancer Res*.

Jhaveri KL, Boni V, Sohn J, Villanueva-Vásquez R, Bardia A, Schmid P, Lim E, Patel JM, Perez-Fidalgo JA, Loi S, Im S-A, Kshirsagar S, Gates MR, Bond J, Eng-Wong J, Chang C-W, Turner NC, Miranda EL, García-Estévez L, and Bellet M (2021) Safety and activity of single-agent giredestrant (GDC-9545) from a phase Ia/b study in patients (pts) with estrogen receptor-positive (ER+), HER2-negative locally advanced/metastatic breast cancer (LA/mBC). *Journal of Clinical Oncology* **39:**1017-1017.

Liang J, Zbieg JR, Blake RA, Chang JH, Daly S, DiPasquale AG, Friedman LS, Gelzleichter T, Gill M, Giltnane JM, Goodacre S, Guan J, Hartman SJ, Ingalla ER, Kategaya L, Kiefer JR, Kleinheinz T, Labadie SS, Lai T, Li J, Liao J, Liu Z, Mody V, McLean N, Metcalfe C, Nannini MA, Oeh J, O'Rourke MG, Ortwine DF, Ran Y, Ray NC, Roussel F, Sambrone A, Sampath D, Schutt LK, Vinogradova M, Wai J, Wang T, Wertz IE, White JR, Yeap SK, Young A, Zhang B, Zheng X, Zhou W, Zhong Y, and Wang X (2021) GDC-9545 (Giredestrant): A Potent and Orally Bioavailable Selective Estrogen Receptor Antagonist and Degrader with an Exceptional Preclinical Profile for ER+ Breast Cancer. *J Med Chem* **64:**11841-11856.

Malhi V, Agarwal P, Gates MR, Liu L, Wang J, De Bruyn T, Lam S, Eng-Wong J, Perez-Moreno P, Chen YC, and Yu J (2023) Optimizing Early-stage Clinical Pharmacology Evaluation to Accelerate Clinical Development of Giredestrant in Advanced Breast Cancer. *Cancer Res Commun* **3:**2551-2559.

Roberts MS, Magnusson BM, Burczynski FJ, and Weiss M (2002) Enterohepatic circulation: physiological, pharmacokinetic and clinical implications. *Clin Pharmacokinet* **41:**751-790.

Roffey SJ, Obach RS, Gedge JI, and Smith DA (2007) What is the objective of the mass balance study? A retrospective analysis of data in animal and human excretion studies employing radiolabeled drugs. *Drug Metab Rev* **39:**17-43.

Schiavon G, Hrebien S, Garcia-Murillas I, Cutts RJ, Pearson A, Tarazona N, Fenwick K, Kozarewa I, Lopez-Knowles E, Ribas R, Nerurkar A, Osin P, Chandarlapaty S, Martin LA, Dowsett M, Smith IE, and Turner NC (2015) Analysis of ESR1 mutation in circulating tumor DNA demonstrates evolution during therapy for metastatic breast cancer. *Sci Transl Med* **7:**313ra182.

Shuet-Hing Lee Chiu and Su-Er W. Huskey (1998). Species Differences in N-Glucuronidation. Drug Metabolism and Disposition. 26: 838-847.

Sung H, Ferlay J, Siegel RL, Laversanne M, Soerjomataram I, Jemal A, and Bray F (2021) Global Cancer Statistics 2020: GLOBOCAN Estimates of Incidence and Mortality Worldwide for 36 Cancers in 185 Countries. *CA Cancer J Clin* **71:**209-249.

Zhang D, Wei C, Hop C, Wright MR, Hu M, Lai Y, Khojasteh SC, and Humphreys WG (2021) Intestinal Excretion, Intestinal Recirculation, and Renal Tubule Reabsorption Are Underappreciated Mechanisms That Drive the Distribution and Pharmacokinetic Behavior of Small Molecule Drugs. *J Med Chem* **64:**7045-7059.

Yang X, Atkinson K, Di L. Novel cytochrome P450 reaction phenotyping for low-clearance compounds using the hepatocyte relay method. Drug Metab Dispos 2016;44(3):460−5.

Zhang C, Su D, Choo CF, Liu L, Bobba S, Jorski JM, Ho Q, Wang J, Kenny JR, Khojasteh SC, Zhang D (2023) Identification of a Discrete Diglucuronide of GDC-0810 in Human Plasma after Oral Administration, Drug Metab Dispos 2023, 51(10): 1284-1294.

DMD Fast Forward. Published on June 4, 2024 as DOI: 10.1124/dmd.124.001688
This article has not been copyedited and formatted. The final version may differ from this version.

Footnotes

a) Genentech, Inc. supported this study.

b) This work has not been presented previously.

c) Reprint requests:

Drug Metabolism and Pharmacokinetics, Genentech, Inc., 1 DNA Way, South San Francisco, CA 94080, USA

d) S.K., J. Y. , M.R.G., S.C.K., V.M., U.O., J.W., S.C., Y.T., D.T., and W.Z. are employees of Genentech, Inc. and hold stock in F. Hoffmann- La Roche Ltd.

Y.C.C., S.Ka., S.M., L.M., and T.D.B. are former employees of Genentech, Inc and L.M., S.M. and T.D.B. hold stock in F. Hoffmann- La Roche Ltd.

e) This work received no external funding.

DMD Fast Forward. Published on June 4, 2024 as DOI: 10.1124/dmd.124.001688
This article has not been copyedited and formatted. The final version may differ from this version.

Figure Legends

Figure 1. Mean (± SD) cumulative recovery of total radioactivity following a single oral dose of [^{14}C]giredestrant (30.8 mg, 105 µCi) given to 6 women of non-childbearing potential expressed as a percentage of the administered [^{14}C] dose in excreta. Triangles and squares represent radioactivity in urine (CumFe(urine)) and feces (CumFe(feces)), respectively. Circles represent the sum of urine and feces (CumFe(total)).

Figure 2. Arithmetic mean (± SD) concentration-time profiles of giredestrant and mean (± SD) total radioactivity in plasma and whole blood following a single oral dose of [^{14}C]giredestrant (30.8 mg, 105 µCi) given to 6 women of non-childbearing potential, on a log-linear scale. The inset shows the linear-linear concentration-time profiles for the first 48 hours post dose.

Figure 3. Arithmetic mean (± SD) plasma concentration-time profiles of giredestrant on a log-linear scale following administration of a single 30 mg dose administered orally as a capsule (triangles) or intravenously as a 30-min infusion (circles).

Figure 4. Representative metabolite radiochromatograms for pooled plasma (upper), urine (middle) and feces (lower) from an individual subject following a single oral dose of [^{14}C]giredestrant.

DMD Fast Forward. Published on June 4, 2024 as DOI: 10.1124/dmd.124.001688
This article has not been copyedited and formatted. The final version may differ from this version.

Figure 5. Proposed metabolic pathway of giredestrant in healthy volunteers following a single 30.8 mg, 105 µCi oral dose. * Indicates the site of the ^{14}C label. F = feces; M = metabolite; *m/z* = mass-to-charge ratio; P = plasma; U = urine; ^{14}C =Carbon-14.

Figure 6. Proposed disposition of giredestrant after oral administration in humans.

DMD Fast Forward. Published on June 4, 2024 as DOI: 10.1124/dmd.124.001688
This article has not been copyedited and formatted. The final version may differ from this version.

Tables

Table 1. Mean pharmacokinetic parameters for giredestrant in plasma and total radioactivity in plasma and whole blood following administration of 30.8 mg, 105 µCi [^{14}C]giredestrant (Part 1).

	Part 1: Mass balance		
PK Parameter	**Giredestrant (Plasma) [N = 6]**	**Total Radioactivity (Plasma) [N = 6]**	**Total Radioactivity (Whole Blood) [N = 6]**
T_{max}[a] (hours)	3.50 (2.00-5.00)	5.00 (2.00-5.00)	5.00 (2.50-5.00)
C_{max} (ng/mL)[b]	74.3 (31.2%)	124 (21.4%)	88.0 (25.8%)
AUC_{0-t} (ng.h/mL)[b]	2600 (43.8%)	4160 (40.3%)	3280 (40.9%)
AUC_{0-inf} (ng.h/mL)[b]	2680 (43.2%)	6480 (39.2%) [n = 3]	NC
$t_{1/2}$ (hours)	42.6 (24.9%)	48.4 (29.4%)	50.8 (46.4%) [n = 3]
CL/F (L/h)	11.5 (43.2%)	NC	NC
Vz/F (L)	705 (20.6%)	NC	NC
WB:P AUC_{0-t}	NA	NA	0.79 (15.9%)

Geometric mean (geometric CV%) are presented unless otherwise indicated. N = number of subjects in the dataset, NC = not calculated.
[a] Median (range) are presented for t_{max}.
[b] Units for total radioactivity are ng equivalent/g for C_{max} and h.ng equivalent/g for AUC

DMD Fast Forward. Published on June 4, 2024 as DOI: 10.1124/dmd.124.001688
This article has not been copyedited and formatted. The final version may differ from this version.

Table 2. Summary of pharmacokinetic parameters of giredestrant following oral administration or 30 min IV infusion of a single 30 mg dose (Part 2).

	Part 2: Absolute bioavailability	
PK Parameter	**IV: 30 mg Solution [N = 10]**	**Oral: 30 mg Formulation18 Capsule [N = 9]**
T_{max}[a] (hours)	0.500 (0.25-0.60)	4.00 (2.00-5.00)
C_{max} (ng/mL)	804 (32.3%)	93.8 (31.1%)
AUC_{0-t} (ng.h/mL)	5700 (33.3%)	3150 (39.2%)
AUC_{0-inf} (ng.h/mL)	5630 (32.5%)	3300 (42.2%)
$t_{1/2}$ (hours)	37.8 (33.9%)	36.4 (21.6%)
CL or CL/F (L/h)	5.31 (32.6%)	9.08 (42.3%)
V_z or V_z/F (L)	266 (21.5%)	476 (24.5%)
F (%)	NA	58.7

Geometric mean (geometric CV%) results are presented unless otherwise indicated. N = number of subjects in the dataset. NA = Not applicable
[a] Median (minimum, maximum) results are presented for t_{max}.

DMD Fast Forward. Published on June 4, 2024 as DOI: 10.1124/dmd.124.001688
This article has not been copyedited and formatted. The final version may differ from this version.

Table 3. Approximate percent of giredestrant and its abundant metabolites in human plasma, urine, and feces following a single oral administration of [^{14}C]giredestrant (30.8 mg, 105 µCi) to women of non-childbearing potential.

Analyte	Biotransformation	% of Total [a]	% of Dose		
		Plasma	Urine [b]	Feces [c]	Total
Giredestrant	Unchanged drug	56.8	1.90	20.0	21.9
M1	Hydroxylation & glucuronidation	6.21	0.0491	ND	0.0491
M2	Glucuronidation	ND	0.167	ND	0.167
M3	Glucuronidation	10.2	2.09	ND	2.09
M5	Hydroxylation	ND	ND	6.85	7.16
M18	Hydroxylation	4.10	0.305		
M26	Oxidation	ND		ND	
M6	*N*-Dealkylation	ND	0.782	ND	5.28
M22	Hydroxylation	6.79		4.50	
M25	Dehydrogenation			ND	
M19	Hydroxylation	ND	ND	7.08	7.08
M20	Hydration	ND	ND		
M21	Hydroxylation	ND	ND	7.76	7.76
M28	Hydration	ND	ND		
M9	Hydroxylation	ND	0.628	6.93	7.56
M8	*N*-Dealkylation	ND	0.0514	7.15	7.20
M11	Oxidative defluorination	ND			
M12	Epimerization	2.43	0.197	1.59	1.79
M27	*N*-Dealkylation	ND	0.276	D	0.276
M23	Dehydrogenation	ND	0.232	ND	0.232
M24	Dehydrogenation	ND	0.358	ND	0.358
M29	Unknown	ND	1.11	2.79	3.90
Total % of dose with parent and metabolites		86.6	8.14	64.7	72.8
% of dose recovered in excreta		NA	9.04	68.0	77.0

D = detected only by mass spectrometry; NA = not applicable; ND = not detected.

[a] % of Total = % of total drug-related material in pooled plasma, 0-48 h for 3 subjects; 0-72 h for 2 subjects; and 0-96 h for 1 subject.

[b] % of Dose = % of the total dose recovered in pooled urine, 0-120 h for 3 subjects; 0-144 h for 2 subjects; 0-168 h for 1 subject.

DMD Fast Forward. Published on June 4, 2024 as DOI: 10.1124/dmd.124.001688
This article has not been copyedited and formatted. The final version may differ from this version.

[c] % of Dose = % of the total dose recovered in pooled feces, 0-408 h for 1 subject; 0-384 h for 1 subject; 0-480 h for 1 subject; 0-216 h for 1 subject; 0-312 h for 1 subject; 0-264 h for 1 subject.

DMD Fast Forward. Published on June 4, 2024 as DOI: 10.1124/dmd.124.001688
This article has not been copyedited and formatted. The final version may differ from this version.

Table 4. Molecular ion and major product ions observed for giredestrant and its metabolites in humans following oral administration.

Analyte	Observed	Theoretical	Mass accuracy	Chemical formula	Matrix[a]	Major Fragment Ions (*m/z*)
	[M+H]$^+$ (*m/z*)		(ppm)			
Giredestrant	523.2488	523.2491	-0.573341	C27H32F5N4O +	P, U, F	MS2: 386.18469 (100), 366.1782, 297.1207, 279.13083, 245.1262, 138.0722, 90.0709
M1	715.2756	715.2761	-0.699031	C33H40F5N4O8 +	P, U	MS2: 539.2440 (100), 402.1806 MS3: 402.1785, 382.1716, 295.1249
M2	699.2806	699.2812	-0.858024	C33H40F5N4O7 +	U	MS2: 386.1840, 314.1044 (100) MS3:314.1044
M3	699.2805	699.2812	-1.001028	C33H40F5N4O7 +	P, U	MS2:386.1847 (100), 314.1054, 138.0723 MS3 366.1788, 297,1200, 277.1130
M5	539.2437	539.244	-0.556334	C27H32F5N4O2 +	F	MS2: 428.1934, 271.10516, 138.0727 (HCD) MS2: 522.1381, 428.1947 (100), 402.17888 (CID)
M6	429.2256	429.2261	-1.164887	C24H28F3N4 +	U	MS2:386.1852 (100), 297.1208, 116.0864, 90.0716, MS3: 366.1782, 297.1197, 277.1139, 257.1064
M8	463.2113	463.2116	-0.647652	C24H27F4N4O +	U, F	MS2: 326.1467 (100), 138.0722 (HCD) MS2: 326.1468 (100) (CID) MS3: 297.1202, 271.1049
M9	539.2436	539.244	-0.741779	C27H32F5N4O2 +	U, F	MS2: 402.17941 (100), 295.1256, 245.1262, 138.0724, 116.08765 (HCD)
M11	521.2529	521.2534	-0.959226	C27H33F4N4O2 +	U, F	MS2:384.1880 (100), 138.0727 (HCD) MS2:384.1889 (100) (CID) MS3: 366.1788, 297.1198, 277.1127, 223.1042 (CID)

DMD Fast Forward. Published on June 4, 2024 as DOI: 10.1124/dmd.124.001688
This article has not been copyedited and formatted. The final version may differ from this version.

M12	523.2489	523.2491	-0.382227	C27H32F5N4O +	P, U, F	MS2: 386.1843 (100), 279.1312, 138.0723 (HCD) MS2: 386.1852 (100), 366.1810 (CID) MS3: 366.1810, 277.1140, 257.1081
M18	539.2436	539.244	-0.741779	C27H32F5N4O2 +	P, U, F	MS2: 402.1793 (100), 295.1246, 245.1264, 138.0723
M19	539.2438	539.244	-0.37089	C27H32F5N4O2 +	F	MS2: 402.1796, 281.11038 (100), 257.1264, 168.0619
M20	541.2592	541.2596	-0.739017	C27H34F5N4O2 +	F	MS2: 430.2108, 271.1422, 257.1264 (100), 138.0724, 116.0867, MS2:168.0618 (HCD) MS2: 430.2113, 404.1956, 257.1266
M21	539.2437	539.244	-0.556334	C27H32F5N4O2 +	F	MS2: 281.1090, 257.1265
M22	539.2436	539.244	-0.741779	C27H32F5N4O2 +	P, U, F	MS2: 386.1842, 154.0672, 116.0862, 90.0715 (HCD) MS2 386.1842 (100) (CID) MS3:386.1841, 297.1203, 289.1135, 277.1139, 257.1075
M23	521.2333	521.2334	-0.191853	C27H30F5N4O +	U	MS2: 386.1851 (100), 366.178, 277.1167 MS3:366.1770, 297.1197, 277.1141, 257.1100
M24	521.2331	521.2334	-0.575558	C27H30F5N4O +	U	MS2: 386.1851 (100), 277.1147 MS3: 366.1783, 297.1201, 277.1140, 257.1078
M25	521.2332	521.2334	-0.383705	C27H30F5N4O +	P, U	MS2:136.566 (HCD), MS2: 386.1843 (100) CID MS3: 366.1766, 297.1208
M26	537.2282	537.2283	-0.186141	C27H30F5N4O2 +	U	MS2: 364.1451 (100) (CID), MS2: 364.1440, 257.1265, 168.0610, 136.0752, 116.0868
M27	408.1695	408.1694	0.244996	C21H22F4N3O +	U	MS2:271.1025 (100), 138.0711

DMD Fast Forward. Published on June 4, 2024 as DOI: 10.1124/dmd.124.001688
This article has not been copyedited and formatted. The final version may differ from this version.

M28	541.2596	541.2596	0	C27H34F5N4 O2 +	F	MS2:386.1839 (100), 138.0724 (HCD), MS2 523.2496 (100), 430.2083 (CID)

P = Plasma, U = Urine, F = Feces

DMD Fast Forward. Published on June 4, 2024 as DOI: 10.1124/dmd.124.001688
This article has not been copyedited and formatted. The final version may differ from this version.

Figure 1.

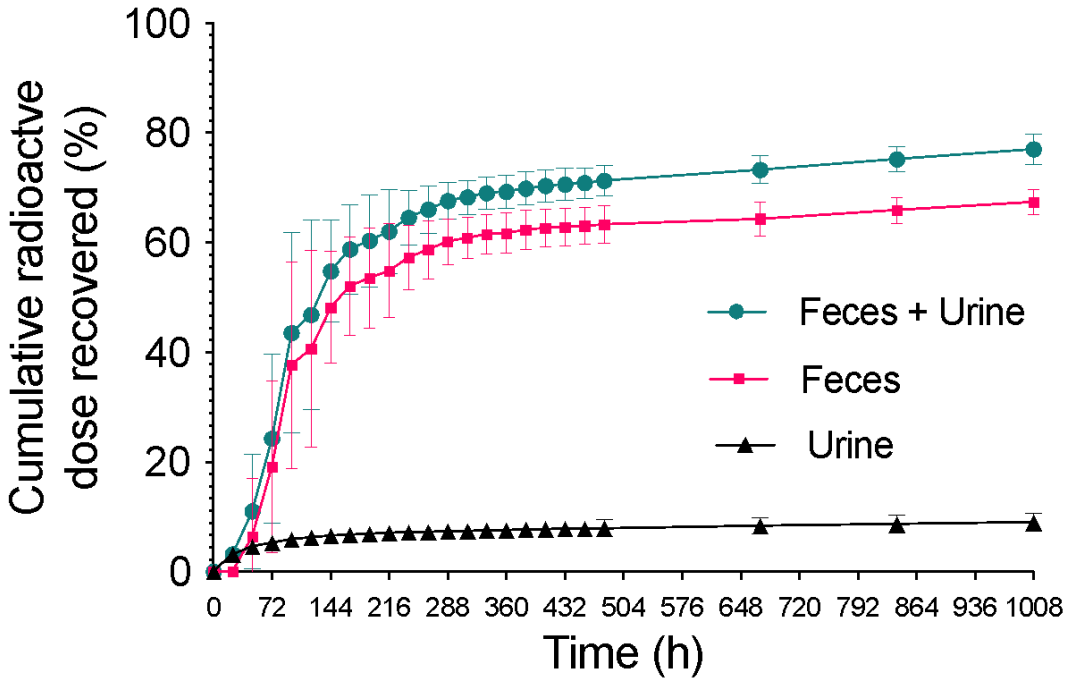

DMD Fast Forward. Published on June 4, 2024 as DOI: 10.1124/dmd.124.001688
This article has not been copyedited and formatted. The final version may differ from this version.

Figure 2.

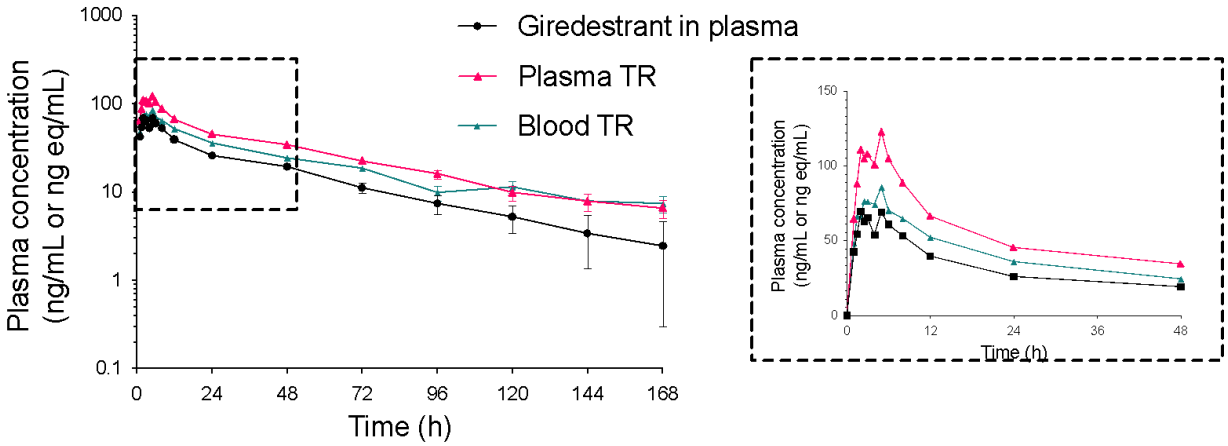

DMD Fast Forward. Published on June 4, 2024 as DOI: 10.1124/dmd.124.001688
This article has not been copyedited and formatted. The final version may differ from this version.

Figure 3

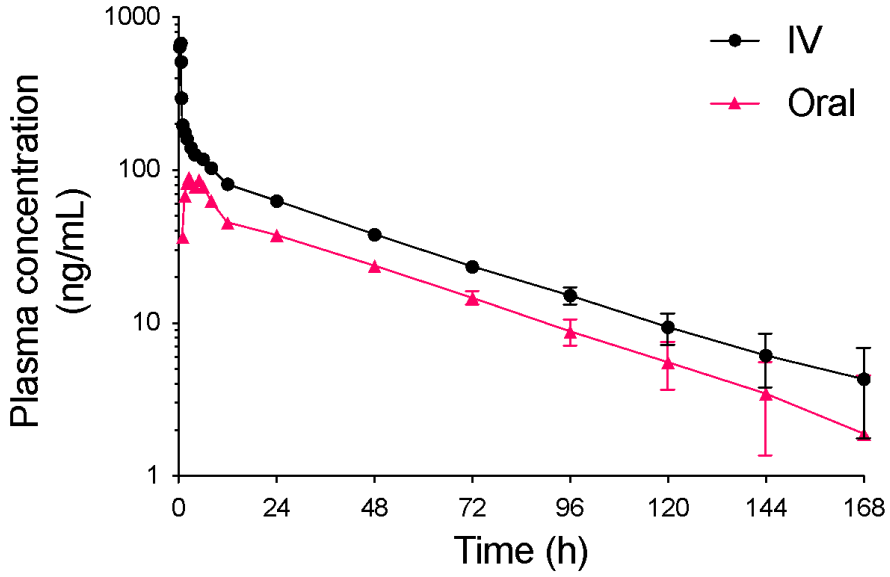

DMD Fast Forward. Published on June 4, 2024 as DOI: 10.1124/dmd.124.001688
This article has not been copyedited and formatted. The final version may differ from this version.

Figure 4

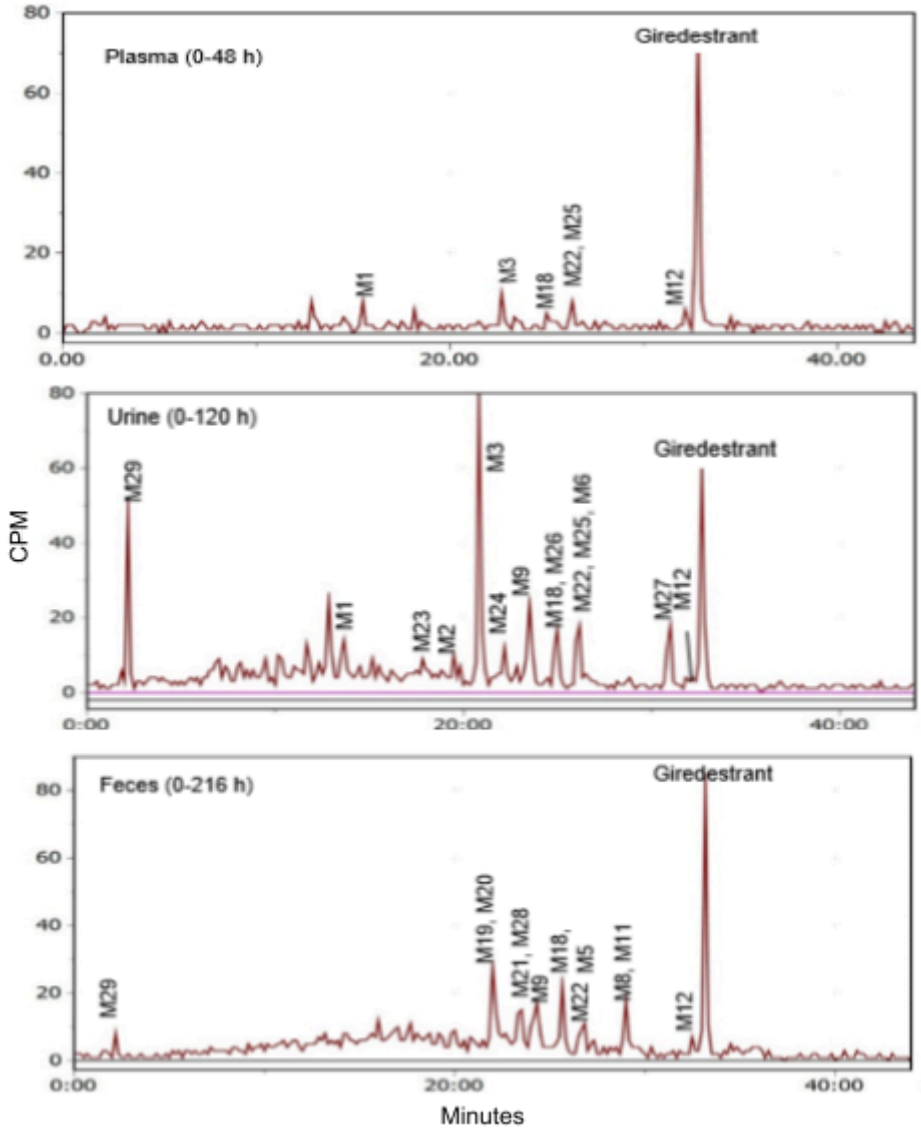

Figure 5

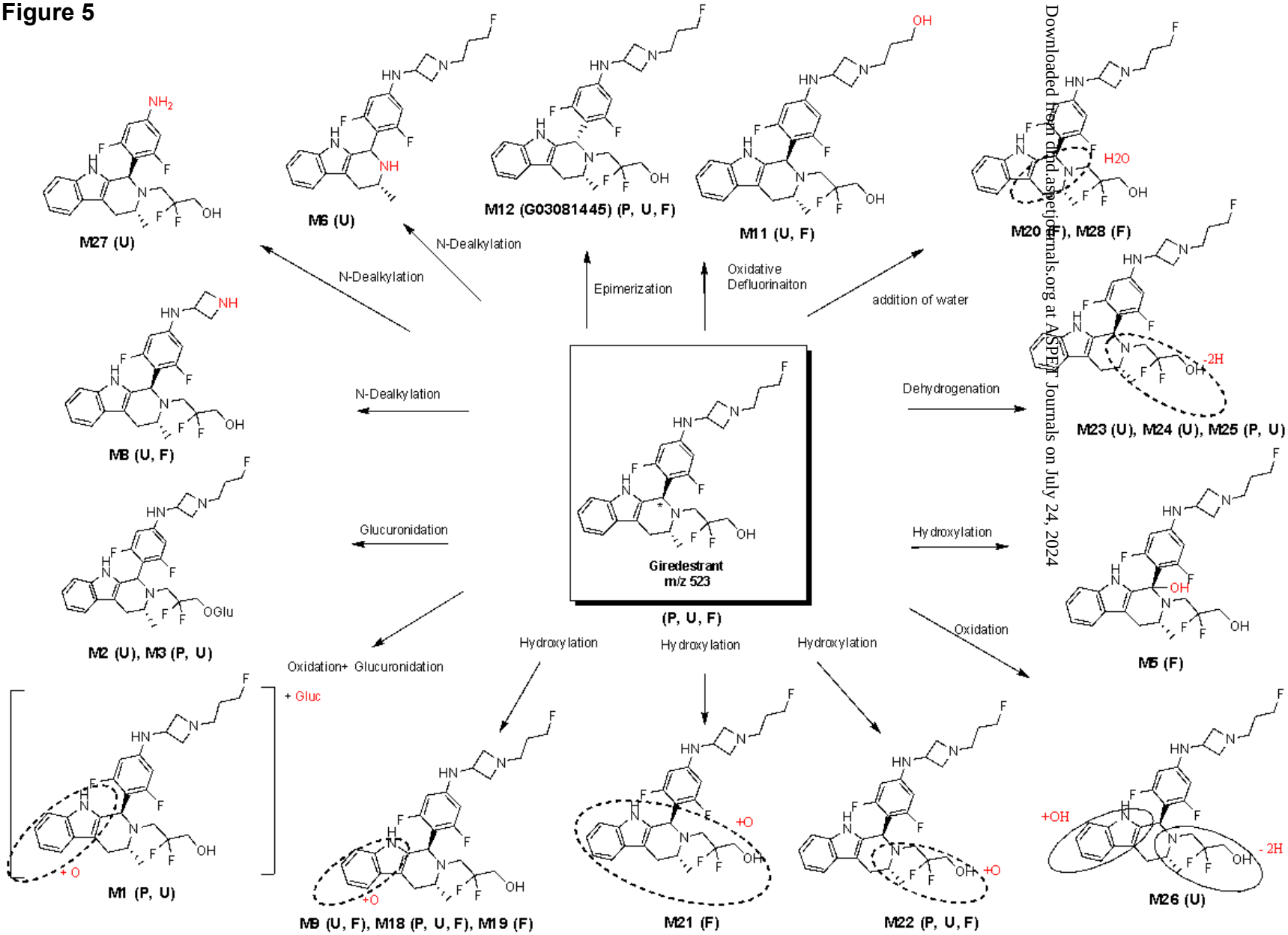

DMD Fast Forward. Published on June 4, 2024 as DOI: 10.1124/dmd.124.001688
This article has not been copyedited and formatted. The final version may differ from this version.

Figure 6